Available online at www.sciencedirect.com
SCIENCE DIRECT®
ELSEVIER
Applied Surface Science 208–209 (2003) 599–603
applied surface science
www.elsevier.com/locate/apsusc

Near-field microscopy investigation of laser-deposited coated conductors

M. Cantoro, N. Coppedè, A. Camposeo, E. Andreoni, M. Labardi, L. Pardi, F. Fuso*, M. Allegrini, E. Arimondo

INFM, Dipartimento di Fisica "Enrico Fermi", Università di Pisa, Via F. Buonarroti 2, I-56127 Pisa, Italy

Abstract

Short-length prototypes of coated conductors consisting of $YBa_2Cu_3O_{7-x}$/yttrium-stabilized zirconia (YBCO/YSZ) bilayers have been fabricated by pulsed laser deposition (PLD) onto biaxially textured NiFe substrates. Scanning probe microscopy has been used for a detailed investigation of local sample properties. In particular, near-field scanning optical microscopy has been exploited to reconstruct a high resolution map of the surface optical scattering properties, which can be related to fluctuations of oxygen stoichiometry at the grain space scale.

Keywords: Pulsed laser deposition; Coated conductors; High temperature superconductors; Near-field scanning optical microscopy

1. Introduction

Since the discovery of high temperature superconductors (HTS), many efforts have been devoted to fabricate long, flexible samples exploitable in current transport applications. Besides powder-based processes, efficient only with Bi- or Tl-based cuprates, the use of more performing HTS, as $YBa_2Cu_3O_{7-x}$ (YBCO), requires film deposition onto flexible metal substrates. Pulsed laser deposition (PLD) is known to be a very efficient technique for deposition of HTS. Even if the debate on its actual industrial potential is still open, PLD is extremely suitable as a method to produce short-length prototypes of coated conductors on flexible substrates.

Some specific problems must be faced within this context. First of all, since electrical transport involves intergrain tunneling, reciprocal alignment and large grain size are desirable to achieve large critical current (J_c) values. In-plane film texturing is thus an important goal for any coated conductor fabrication method, typically involving deposition of one or more dielectric layers acting as an interdiffusion barrier and as a template for the subsequent growth of the HTS film. Several approaches have been recently proposed to attain texturing, which can be grossly divided in two main categories, depending on whether a pre-textured metal substrate is used, or not. Ion-beam assisted deposition (IBAD [1]) and inclined substrate deposition (ISD [2]) may be used with non-textured substrates, but suffer drawbacks in terms of growth rate (IBAD) and compatibility with PLD (ISD). Processes starting from rolling-assisted biaxially textured substrates (RABiTS [3]) overcome this limitation, but impose strict requirements on the substrate material.

* Corresponding author. Tel.: +39-0502214305; fax: +39-0502214333.
E-mail address: fuso@df.unipi.it (F. Fuso).

0169-4332/02/$ – see front matter
doi:10.1016/S0169-4332(02)01398-3

Indeed, the second class of problems in PLD of coated conductors involves some specific features of the metal substrate. High degree of substrate texturing can be attained by relatively simple metallurgical methods (e.g. cold-rolling, followed by annealing) in pure Ni and Ni-alloys, often preferable for their improved mechanical strength. Furthermore, some alloys, including NiFe, are appealing also from the economical point of view, long tapes being commercially available. On the other hand, besides the magnetic character of the alloy, limiting the range of possible applications, surface oxidation processes, with consequent detrimental effects, demand a special care to design the deposition process and to find out suitable operating parameters.

In this paper, we report on PLD of YBCO/yttrium-stabilized zirconia (YSZ) bilayers on biaxially textured NiFe (50–50 at.% 10 mm × 10 mm × 25 μm) by a simple, economic, and eventually scalable process. To this aim, a single buffer layer has been used and, contrary to other examples reported in the literature [4], no forming (i.e. reducing) environment gas has been employed. Furthermore, no attempt to induce preliminary surface oxidation of the substrate in controlled conditions, leading to textured polycrystalline oxide growth (see, e.g. [5]), has been applied. Our samples have been analyzed by a variety of methods, including an innovative technique based on near-field scanning optical microscopy (NSOM).

2. Experimental setup

We used a conventional apparatus for PLD based on a commercial XeCl excimer laser and a deposition chamber equipped with a multi-target carrousel holder. We explored a wide range of parameters during deposition of both YSZ and YBCO. Best samples were obtained by depositing YSZ in high vacuum ($P < 10^{-6}$ mbar), whereas growth of orthorombic YBCO required the presence of a molecular oxygen environment, at typical pressures around 0.3 mbar. Laser fluence and target/substrate distance were 4 J/cm^2 and 33 mm, respectively. Substrate temperature and thermal treatment of the sample after deposition were critical to attain superconductivity. Typically, both layers were deposited at 800 °C, and, after the deposition, sample cooling at 10 °C/min in the presence of O_2 at 0.3 mbar was adopted to minimize crack formation. Film thickness, depending on the number of laser shots, was 0.8–1.0 μm for both layers.

Investigation of the electrical properties was performed by a cryogenic 4-probe system. Laser patterning was employed to define current flow patterns on the film surface, in order to estimate J_c. The same excimer laser used for PLD was focused on the sample surface in air, and the plume fluorescence emission of some selected elemental lines was analyzed on a single-shot basis to control complete removal of the HTS layer. Regular stripes with a minimum width around 0.1 mm and length of a few mm could be obtained.

Microscopic analysis of the samples has been performed by using a home-made NSOM setup, basically described elsewhere [6]. Briefly, a commercial tapered and metallized optical fiber, with an apical aperture with diameter $a \sim 50$ nm, is used as a quasi-point-like emitter of a non-propagating e.m. field, which extinguishes on a scale $\sim a$. The sample is placed under the fiber tip, and scanning in the horizontal plane is accomplished by a piezoelectric translator. During the scan, tip/sample distance d is kept within the near-field range (typically, $d < 10$ nm) by a system based on shear-force detection [6]. The error signal of the feedback circuit used to stabilize the distance is continuously acquired in order to have a simultaneous map of the surface topography. Ar^+ or HeNe laser light at 488 or 633 nm, respectively, is coupled to the fiber and the radiation locally scattered by the sample is collected and detected in the far-field, at 45° off surface. Furthermore, control and modulation of the light polarization may be applied in both excitation and detection in order to study dichroic or birefringence behavior of the sample, not applied in data presented here.

3. Results and discussion

The structural analysis of our samples, already presented in [7], showed that rather good results can be achieved for a suitable choice of deposition parameters. In particular, X-ray diffraction patterns revealed the occurrence of a correct growth of orthorombic YBCO along the c-axis, whereas X-ray pole figures demonstrated a high degree of biaxial texturing

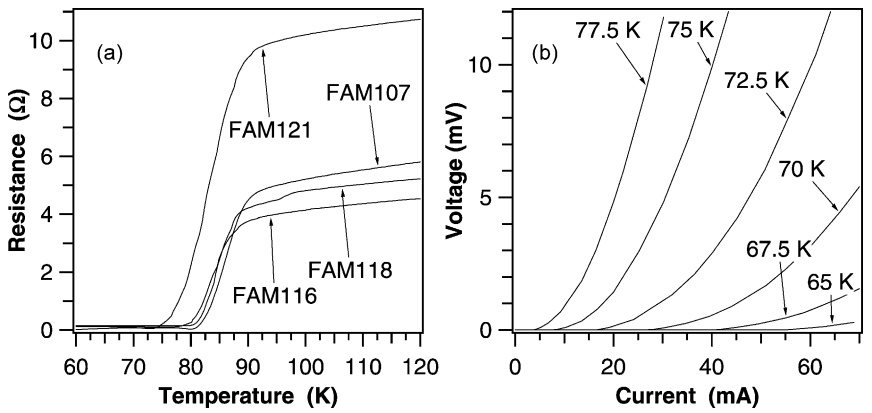

Fig. 1. (a) Resistance vs. temperature plots for some samples (FAM107, 116, 118 grown in similar conditions at the substrate temperature $T = 800$ °C, FAM121 grown at a larger substrate temperature, $T = 820$ °C); (b) voltage vs. current plots for sample FAM116 measured at different temperatures, as shown close to each curve, in a stripe with an estimated cross-section of 10^{-2} mm^2; the corresponding J_c value at 77 K is around 10 kA/cm^2. We note that the uncertainty in the film temperature is around 1 K in the actual conditions of the measurements (temperature sensor on the cryostat head).

(up to 85%) with a rather low mosaic spread (pole width <10°). X-ray signals ascribed to Ni- or Fe-oxides were almost negligible, at least by keeping O_2 pressure in the deposition chamber in the tenths of mbar range, which, in turn, ensured YBCO crystallization in the orthorombic phase.

On the contrary, electrical transport properties turned out not completely satisfying. For instance, Fig. 1(a) shows the resistance versus temperature behavior of a few samples: as in [4], the transition appears broader than in YBCO films deposited onto single crystal substrates. Comparison between results for a set of samples demonstrates repeatability of the process and sensitivity on the parameters. On some samples, the critical current density J_c at zero magnetic field was estimated by defining linear stripes for current flow, with known dimensions. Voltage versus current measurements across these stripes were performed as a function of temperature (Fig. 1(b)). We set a voltage value roughly corresponding to the actual noise of the measurement (100 μV), above which we inferred the normal state was reached. Current density was then derived by simply dividing the measured current by the geometrical area of the current flow tube. We stress that the so-obtained value should be intended as an underestimate of J_c, since we cannot rule out effects of the laser patterning on the border of the stripes, which could lead to destroy superconductivity in that region of the film, thus reducing the effective width of the stripe. We estimated values around 10 kA/cm^2 at 77 K, well below the performance offered by YBCO films deposited onto single crystal substrates.

The substantial discrepancy between structural and functional results, reported, as already mentioned, also by other authors [4], gave us motivations for a detailed microscopic analysis of our samples. For some choice of deposition parameters (e.g. O_2 pressure, substrate temperature or cooling ramp), we found a remarkable occurrence of substrate oxidation, leading to dramatic effects, as crack formation and peel-off of the deposited layers. However, films grown with correct parameters did show a relatively good morphology, as ascertained by atomic force microscopy [7], with a rather compact structure of grains sized in the range between hundreds of nanometer and a few micrometer. Thus, more subtle microscopic features must be investigated to explain our macroscopic findings.

Within this context, NSOM offers the unique opportunity to study surface optical properties with a space resolution below the diffraction limit (around one-half the wavelength used in the investigation), as needed to get reliable information on a single YBCO grain. It is known by conventional (macroscopic) ellipsometry [8] that YBCO reflectivity is a strong function of the oxygen content, which, in turn, affects structure and electrical properties of the material. We note that

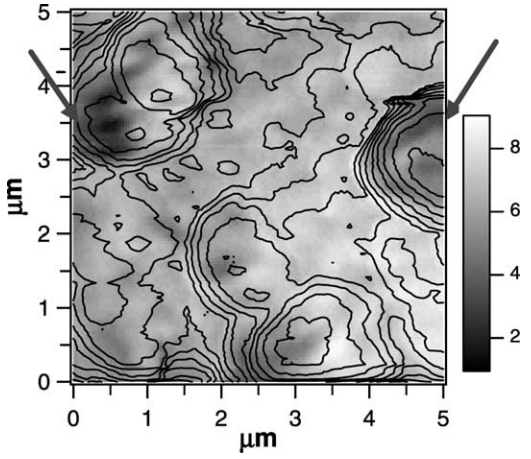

Fig. 2. NSOM image of sample FAM109 (grown in conditions similar to FAM121), with superimposed the contour plot of the topography (dynamical range 0–700 nm). A reverse gray scale has been used in the representation , colors black and white meaning low and high levels of scattered optical radiation, as in the color table. The arrows point to regions where optical and topography maps appear uncorrelated each other.

NSOM was already used to analyze the surface of HTS films [9,10]. However, in our technique we specifically address the point of local variation of oxygen stoichiometry which can occur in the top layer of coated conductors.

The first issue to be carefully examined in NSOM analysis is the relationship between topography and radiation scattering. Indeed, the intensity of the reflected light depends on the actual tip/sample distance and on the angle between the imaged portion of sample and the collection optics. In order to minimize the related effects, we have developed and applied a linear deconvolution method, which was verified on planar test samples.

An example of deconvoluted NSOM scattering image, acquired with 488 nm excitation on sample FAM109 (grown in conditions similar to those of FAM121, see Fig. 1), is shown in Fig. 2. Superimposed to the image is a contour plot of the surface topography, acquired simultaneously during the NSOM scan, which allows us to identify the presence of relatively large grains (size 1–2 µm) with a mostly polygonal shape. Traces of topographical variations remain in the optical image, especially at the grain borders. However, features appear which are not directly correlated with the topography, as those observed in the flat top of the grains (see arrows in Fig. 2). Some of the features observed in the optical image have a sub-wavelength extension, confirming the resolution of the near-field method. These features can be ascribed to local variations of the optical properties, which, in turn, can be related to fluctuations in surface stoichiometry, or to the presence of impurities.

In the variety of results that we have acquired, to be presented in details elsewhere, a remarkable finding is that quite often, especially in samples characterized by

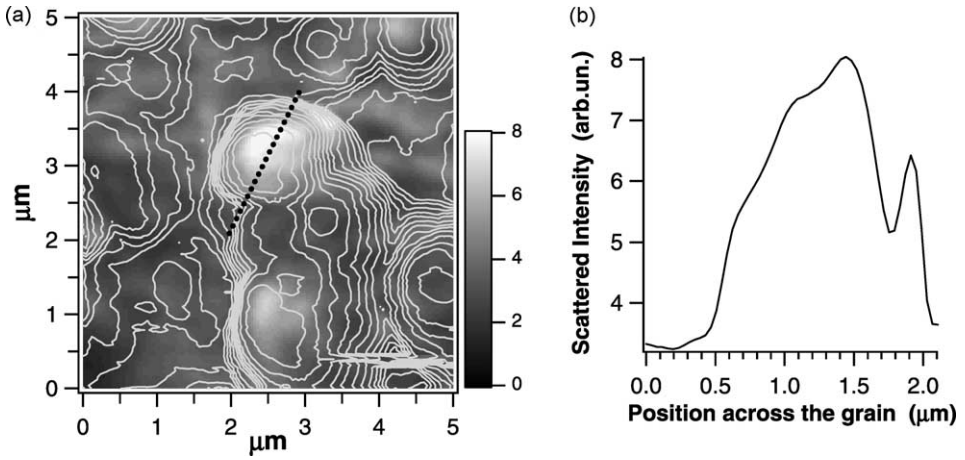

Fig. 3. (a) NSOM image of sample FAM107, with superimposed the contour plot of the topography (dynamical range 0–500 nm); (b) line profile analysis along the row marked with a dashed line in panel (a).

poor electrical properties, the scattered NSOM signal from an YBCO grain shows a peculiar behavior, decreasing from the center towards the border. Fig. 3 reports an example (panel (a)), along with the corresponding line profile analysis (panel (b)). According to the macroscopic data of YBCO reflectivity [8], our results suggest that the oxygen content is in this case a function of the position across the grain, with a decreasing behavior when moving from the center to the border. In other words, probably as a consequence of the mechanical stress suffered by the YBCO layer growing on top of YSZ, oxygen could be released by the outer surface of the grain [11]. Thus, an annular region with an oxygen deficiency, and a subsequent non-superconductive character, would occur surrounding the grain, so decreasing the efficiency of the intergrain tunneling involved in electrical transport on the macroscopic scale. Further considerations on our measurements will be presented elsewhere. However, we point out that such a behavior was not clearly observed in the analysis of YBCO deposited onto single crystal substrates with optimal transport properties, so that it may be taken as a distinctive feature of our coated conductor samples.

4. Conclusions

We have applied PLD to fabrication of coated conductors with a YBCO/YSZ architecture onto biaxially textured NiFe substrates. The whole process has been inspired by the maximum degree of simplicity and scalability, having in mind an industrial-oriented application. Results are controversial. Structural properties are compatible with the proposed application, but the electrical behavior is not fully satisfying, as reported by other authors working with a similar substrate, but with a more sophisticated process. In order to unravel the peculiar features of our samples, we have developed a microscopical method based on NSOM. The main findings of the NSOM analysis suggest the occurrence of local fluctuations in the oxygen content, with a peculiar behavior across a single YBCO grain, which might contribute to explain the observed macroscopical behavior.

Acknowledgements

Work supported by CNR through Progetto ‘‘Applicazioni della Superconduttività ad Alta T_c’’.

References

[1] Y. Ijima, N. Tanabe, O. Kohno, Y. Ikeno, Appl. Phys. Lett. 60 (1992) 769.
[2] K. Hasegawa, K. Fujino, H. Mukai, M. Konishi, K. Hayashi, K. Sato, S. Honjo, Y. Sato, H. Ishii, Y. Iwata, Appl. Supercond. 4 (1996) 487.
[3] A. Goyal, D.P. Norton, J.D. Budai, M. Paranthaman, E.D. Specht, D.M. Kroeger, D.K. Christen, Q. He, B. Saffian, F.A. List, D.F. Lee, P.M. Martin, C.E. Klabunde, E. Hartfield, V.K. Sikka, Appl. Phys. Lett. 69 (1996) 1795.
[4] R.I. Tomov, A. Kursumovic, M. Majoros, D.-J. Kang, B.A. Glowacki, J.P. Evetts, Supercond. Sci. Technol. 15 (2002) 598.
[5] S. Ceresara, V. Boffa, F. Fabbri, P. Scardi, Int. J. Mod. Phys. B 13 (1999) 1035.
[6] P.G. Gucciardi, M. Labardi, S. Gennai, F. Lazzeri, M. Allegrini, Rev. Sci. Instrum. 68 (1997) 3088.
[7] M. Cantoro, N. Coppedè, A. Camposeo, M. Labardi, L. Pardi, F. Fuso, M. Allegrini, E. Arimondo, A. Baldini, A. Botarelli, M. Lancia, G. Masciarelli, Int. J. Mod. Phys. B, 2002, in press.
[8] J. Kircher, M.K. Kelly, S. Rashkeev, M. Alouanim, Phys. Rev. B 44 (1990) 217.
[9] J.D. Pedarnig, H. Gottlich, R. Rossler, Appl. Phys. A 67 (1998) 403.
[10] S.H. Huert, M.P. Taylor, H.D. Hallen, Appl. Phys. Lett. 77 (2000) 2127.
[11] P.M. Grant, Nature 407 (2000) 139.